Measuring postquench entanglement entropy through density correlations

Adrian Del Maestro, 1,2 Hatem Barghathi, 1 and Bernd Rosenow

¹Department of Physics and Astronomy, University of Tennessee, Knoxville, Tennessee 37996, USA

²Min H. Kao Department of Electrical Engineering and Computer Science, University of Tennessee, Knoxville, Tennessee 37996, USA

³Institut für Theoretische Physik, Universität Leipzig, D-04103 Leipzig, Germany



(Received 8 December 2021; revised 17 March 2022; accepted 22 March 2022; published 26 April 2022)

Following a sudden change of interactions in an integrable system of one-dimensional fermions, we analyze the dependence of the static structure factor on the observation time after the quantum quench. At small waiting times after the quench, we map the system to noninteracting bosons such that we are able to extract their occupation numbers from the Fourier transform of the density-density correlation function, and use these to compute a bosonic entropy from a diagonal ensemble. By comparing this bosonic entropy with the asymptotic steady-state entanglement entropy per fermion computed with exact diagonalization, we find excellent agreement.

DOI: 10.1103/PhysRevResearch.4.L022023

Recent experimental and theoretical advances have elucidated the time evolution of spatial entanglement for a system that remains in a pure quantum state after a sudden change in the Hamiltonian. In the steady-state asymptotic limit, the entanglement entropy becomes extensive in the size of a spatial subsystem [1,2], and plays the role of a thermodynamic entropy arising from a microcanonical ensemble with the same energy density [3–6].

Here, we show that the entanglement entropy density after an interaction quench can be obtained from the diagonal ensemble density matrix [6–10] of noninteracting bosons, whose properties can be determined from density-density correlations. Such correlations are readily accessible via current experimental technologies in a quantum gas via Bragg spectroscopy [11–14] without the need to directly measure coherences. This result presents a complementary route to the experimental measurement of entanglement entropy in quantum systems that is not based on the creation of replicas [2,15–17], and highlights the role played by entanglement dynamics in generating an effective thermodynamic description that underlies our current framework of quantum statistical mechanics.

The study of quantum quenches in one-dimensional systems has been very fruitful in understanding thermalization in closed quantum systems [8,18–25]. We here consider an integrable model of interacting spinless fermions in one spatial dimension and obtain an explicit formula for the time dependence of the postquench static structure factor via bosonization. The occupation numbers of bosonic modes can then be used to compute the entropy within the framework of an effective diagonal ensemble. This entropy is compared

Published by the American Physical Society under the terms of the Creative Commons Attribution 4.0 International license. Further distribution of this work must maintain attribution to the author(s) and the published article's title, journal citation, and DOI.

to the extensive asymptotic spatial entanglement entropy found via large-scale exact diagonalization of the underlying fermions and we find excellent agreement between the two. Our results can be readily adapted to an experimental protocol for measuring the entanglement after a quantum quench in trapped one-dimensional quantum gases.

Fermions with finite-range interactions. In equilibrium, all thermodynamic quantities characterizing interacting fermions in one dimension can be computed via a mapping to a thermal ensemble of noninteracting bosons [26,27]. In particular, the thermal bosonic entropy can be directly computed from knowledge of the average bosonic mode occupancy. In the following, we describe how this concept can be generalized to a nonequilibrium situation after a quantum quench, and how the bosonic mode occupancies can be determined experimentally. The starting point is an analysis of the Fourier transform of the density-density correlation function, known as the static structure factor.

We consider a system of N fermions on a one-dimensional lattice with L sites, described by a Hamiltonian $H_0 + \theta(t)H_1$, which undergoes a quantum quench at time t=0. The fermions are described by creation and annihilation operators c_i^{\dagger} , c_i with commutation relations $\{c_i, c_j^{\dagger}\} = \delta_{ij}$. One can then define the density operator $\rho_i = c_i^{\dagger}c_i$, with an average density $\rho_0 = N/L$. We now consider the density operator $\rho_i(t)$ in the Heisenberg picture, evaluated at time t after the quantum quench, and define the density-density correlation function,

$$g_2(i-j;t) = \frac{\langle \rho_i(t)\rho_j(t)\rangle}{\rho_0^2} - \frac{\delta_{i,j}}{\rho_0}.$$
 (1)

We stress that g_2 is an equal-time correlation function, with t denoting the observation time after the quantum quench. Via a Fourier transform we obtain the static structure factor s(q;t) after observation time t as

$$s(q;t) = 1 + \rho_0 \sum_{r=0}^{L/2-1} [g_2(r;t) - 1]e^{-iqr}.$$
 (2)

Bosonization methods can be used to obtain a prediction for the observation time dependence of the structure factor, which in turn allows one to extract the occupation numbers of bosonic modes after the quantum quench. The result of such a calculation for a Luttinger liquid (LL) with a quadratic Hamiltonian (shown in the Supplemental Material [28]) is

$$s_{\rm LL}(q;t) = s_{\rm LL}(q)[2\langle n_q \rangle + 1 + \sinh(2\beta_q)\cos(2\omega_q t)], \quad (3)$$

where β_q parametrizes the transformation between free fermions and the eigenstates of the postquench Hamiltonian, and ω_q is the dispersion relation of density waves after the quantum quench. Above, $s_{\rm LL}(q)$ is the equilibrium ground-state static structure factor, which at low energies and long wavelengths is given by [27]

$$s_{\rm LL}(q) \underset{q \to 0}{=} \frac{K|q|}{2k_{\rm F}}.\tag{4}$$

The Luttinger parameter K is related to the strength of interactions and $k_{\rm F}$ is the Fermi wave vector. Considering the ratio $s_{LL}(q;t)/s_{LL}(q)$ allows us to extract the bosonic occupation $\langle n_q \rangle$ from the time-independent part of this expression. For a LL with a pointlike (i.e., momentum-independent) interaction, one finds that $\langle n_q \rangle \equiv \langle n_{q=0} \rangle = \frac{1}{4}(K + \frac{1}{K} - 2)$ is independent of q. For more realistic Hamiltonians, the interaction is momentum dependent, giving rise to a q-dependent bosonic mode occupancy $\langle n_q \rangle$ after the quench. In addition, band curvature effects lead to a coupling between bosonic modes [29-32], such that the mode occupancy $\langle n_q \rangle$ is no longer a constant of motion but acquires a time dependence. We expect these nonlinear effects to be suppressed by at least a factor of $\langle n_q \rangle$, which is small (see Fig. 3). In our numerical analysis, we use Eq. (3) only for short times t after the quench, for which the mode coupling has not yet had any appreciable

Staying within the Luttinger model, the Hamiltonian is quadratic in boson operators and thus the entropy of the density wave excitations can be computed exactly. In this picture, the bosonic mode occupation operator n_q commutes with the postquench Hamiltonian, and thus all its higher-order correlations are time-independent conserved quantities. When computing them using a squeezing transformation [18,33,34] between the original and postquench bosons [28], one finds, for instance, $\langle n_q^2 \rangle = 2 \langle n_q \rangle^2 + \langle n_q \rangle$. This hierarchy can be described by a diagonal ensemble with a density matrix

$$\rho_{\text{diag}} = e^{-\sum_{q>0} \lambda_q n_q} \delta_{n_q, n_{-q}}, \tag{5}$$

where λ_q is an effective temperature chosen to fix $\langle n_q \rangle$ [8]. This ensemble preserves correlations between modes with opposite momenta, $\langle n_q n_{-q} \rangle \equiv \langle n_q n_q \rangle$, arising from interactions between them. The density matrix in Eq. (5) is not equivalent to the generalized Gibbs ensemble density matrix [4,6,21,35]; it is constructed from nonlocal degrees of freedom and does not include any information about nonparticle conserving correlations [21].

We compute the bosonic entropy via $S_b = -2 \operatorname{Tr} \rho_{\text{diag}} \log \rho_{\text{diag}}$, with the factor of 2 originating from the diagonal nature of the ensemble [9,10]. Exploiting the fact that there are no interactions between the bosonic density

waves, their entropy density is

$$\mathfrak{s}_b \equiv \frac{S_b}{N} = \frac{2}{N} \sum_{q>0} \left[(1 + \langle n_q \rangle) \ln(1 + \langle n_q \rangle) - \langle n_q \rangle \ln\langle n_q \rangle \right]. \tag{6}$$

Here, the sum runs over positive momenta only due to the constraint between modes in Eq. (5), enforcing the same occupancy of positive and negative q modes and thus the modes with negative momenta do not contribute.

In the following, we argue that the postquench entropy Eq. (6) evaluated for the LL model is equal to the density of asymptotic spatial entanglement entropy for the underlying fermions. This is motivated by the result that in equilibrium and at low temperatures, the bosonic entropy is equal to the thermodynamic entropy of the microscopic interacting fermion system [27]. For an integrable system after a quantum quench, the Yang-Yang entropy computed from the occupation numbers of the exact eigenstates of the interacting system is known to agree with the asymptotic steady-state spatial entanglement entropy per particle [22,24,36], computed as the von Neumann entropy

$$S(t;\ell) = -\text{Tr}[\rho_{\ell}(t) \ln \rho_{\ell}(t)], \tag{7}$$

where $ho_\ell(t)$ is the postquench spatially reduced density matrix

We define a quadratic Luttinger model by demanding that it faithfully reproduces the first few oscillations of the static structure factor as a function of waiting time after the quench. We then compute the entropy of this LL model from its asymptotic diagonal ensemble density matrix. In this way, we approximate the exact eigenstates of an interacting fermion model with those of the Luttinger model, and propose in analogy to the Yang-Yang entropy that Eq. (6) computed from the LL mode occupancies is equal to the density of spatial entanglement. For the LL model, $\langle n_q \rangle$ can be determined in an unambiguous manner from the structure factor by using Eq. (3). The above approximation seems reasonable as both the microscopic and the LL model are similarly constrained integrable models. We test this hypothesis with an extensive numerical experiment, and find excellent agreement between the postquench diagonal ensemble entropy Eq. (6) and the asymptotic spatial entanglement entropy from Eq. (7).

Demonstration for a lattice model. We consider an integrable one-dimensional model of spinless fermions described by

$$H = -J \sum_{i=1}^{L} (c_i^{\dagger} c_{i+1} + \text{H.c.}) + \theta(t) V \sum_{i=1}^{L} c_i^{\dagger} c_i c_{i+1}^{\dagger} c_{i+1}, \quad (8)$$

where the first term corresponds to free fermions (H_0) , and the second term to a nearest-neighbor interaction V, switched on at time t=0 [H_1 with $\theta(t)$ the Heaviside step function]. The equilibrium phases of the postquench Hamiltonian at half filling (N=L/2) are known via a mapping to the XXZ spin model [37,38]. For -2 < V/J < 2 the ground state is a quantum liquid, with a first-order transition at V/J = -2 to a phase-separated solid (ferromagnet in the spin language). At V/J = 2 there is a continuous transition to an insulating state with staggered density wave order (antiferromagnet in the

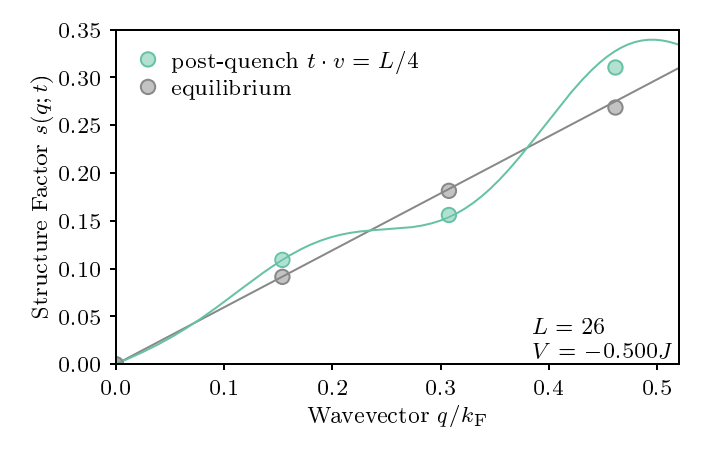


FIG. 1. Comparison between equilibrium and postquench structure factor. The static structure factor at small wave vectors for a quantum quench to interaction strength V=0.5J at fixed time $t \cdot v = L/4$ (corresponding to an extremum of the oscillations) deviates significantly from its equilibrium counterpart. The solid lines correspond to Luttinger-liquid predictions as defined in Eqs. (4) and (2) using values of K and v computed from Eq. (9).

XXZ model). The quantum liquid regime at low energies is described by the linear hydrodynamics of the Luttinger model with interaction parameters K and velocity v given by

$$K = \frac{\pi}{2\cos^{-1}\left(-\frac{V}{2J}\right)}, \quad \frac{v}{J} = \pi \frac{\sqrt{1 - (V/2J)^2}}{\cos^{-1}(V/2J)}, \quad (9)$$

where the lattice spacing has been set to unity.

At t=0, the ground state $|\Psi_0\rangle$ of Eq. (8) corresponds to noninteracting fermions, and after the sudden quench, the initial state evolves according to $|\Psi(t)\rangle = e^{-iHt}|\Psi_0\rangle$ which is obtained via numerical exact diagonalization for system sizes up to L=26 by exploiting translation, reflection, and particle-hole symmetries of the microscopic Hamiltonian. All postquench observables are computed from $|\Psi(t)\rangle$ or its associated density matrix $\rho = |\Psi(t)\rangle\langle\Psi(t)|$. All code, data, and scripts necessary to reproduce the results of this work are included in an online repository [39].

In Fig. 1 we compare the postquench static structure factor Eq. (2) at a fixed time t (corresponding to its first extremum for $q = 2\pi/L$), with the time-independent structure factor of an associated equilibrium model having the same nearest-neighbor interaction strength (V = -0.5J here) for L=26 sites at half filling. In both cases, data points (circles) were obtained via exact diagonalization, and the theoretical Luttinger-liquid predictions for small q (solid lines) were computed from Eqs. (3) and (4). We have used the Bethe ansatz solution to convert the interaction strength to the effective parameters of the Luttinger model where $\langle n_q \rangle \equiv \langle n_{q=0} \rangle =$ $\frac{1}{4}(K^{+}+K^{-1}-2)$, $\sinh 2\beta_{q} \equiv \frac{1}{2}(K-K^{-1})$, and $\omega_{q} = vq$ as discussed in the Supplemental Material [28]. At small wave vectors, the exact diagonalization results are in very good agreement with the Luttinger-liquid predictions, both in equilibrium and for a quantum quench, while deviations start to increase as the wave vector approaches a finite fraction of $k_{\rm F}$.

Extracting the bosonic momenta distribution. Exact diagonalization results for the postquench time dependence of the

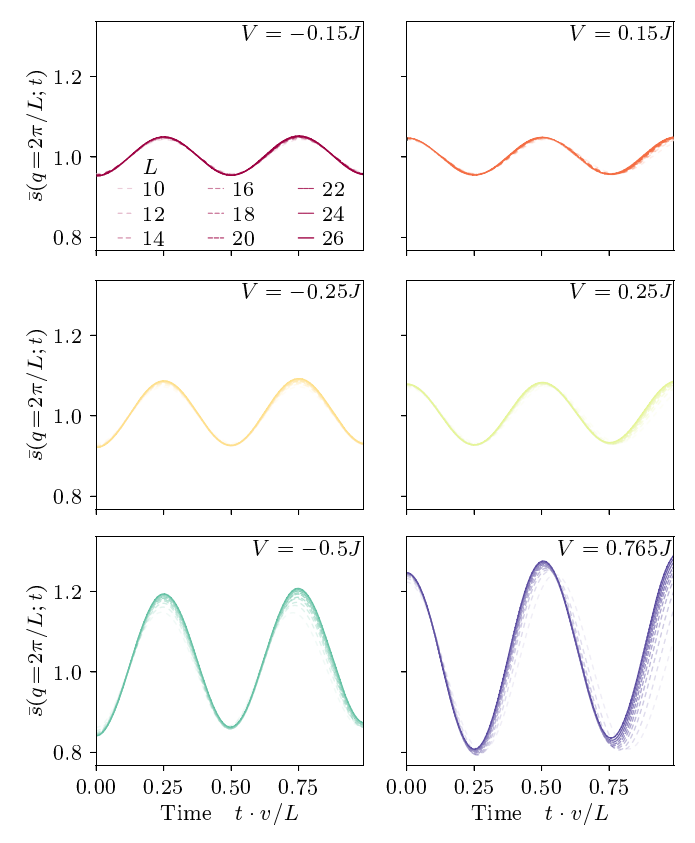


FIG. 2. Exact diagonalization results for the observation time dependence of the normalized static structure factor $\bar{s} = s(q;t)/s_{\rm eq}(q)$ after a quantum quench at the smallest value of momentum $q=2\pi/L$. Panels correspond to different final interaction strengths V. After a spline interpolation, the period of the oscillation is determined, allowing for the determination of $\langle n_q \rangle$, K, and v by taking into account the first one and a half periods. Time after the quench is measured in units of the inverse velocity given in Eq. (9). Dash length and transparency indicate different system sizes.

static structure factor [Eq. (2)] $\bar{s}(q;t) \equiv s(q;t)/s_{eq}(q)$ normalized by its equilibrium ground-state value $s_{eq}(q)$ are shown in Fig. 2 for a number of interaction strengths and system sizes for the smallest admitted wave vector, $q = 2\pi/L$. In practice, the appearance of finite-size effects is suppressed by rescaling the dimensionless time by the system size L, to achieve data collapse. The oscillatory structure seen in Fig. 2 predicted by the Luttinger-liquid result $s_{LL}(q;t)/s_{LL}(q)$ in Eq. (3) can be exploited to recover the parameters of the underlying microscopic model as well as the q-dependent boson occupations $\langle n_q \rangle$ without the need for nonlinear fitting. For each interaction strength V, system size L, and wave vector q, we perform a cubic spline interpolation to the discrete time sampled $\bar{s}(q;t)$. The frequency of oscillations ω_q can then be independently determined from the location of the first three nontrivial extrema, corresponding to 1/2, 1, and 3/2 periods, respectively. Integrating $\bar{s}(q;t)$ over these respective times yields

$$I_n(q) = \frac{\omega_q}{n\pi} \int_0^{n\pi/\omega_q} dt [\bar{s}(q;t) + \delta \cdot t] = 1 + 2\langle n_q \rangle + \delta \frac{n\pi}{2\omega_q},$$
(10)

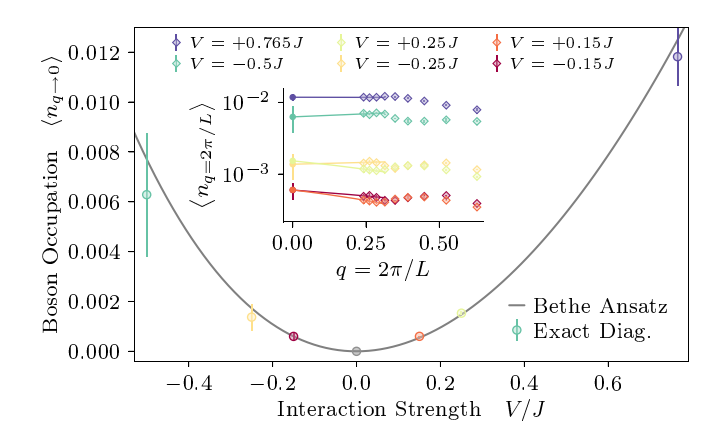


FIG. 3. Bosonic density mode occupations. The expectation value $\langle n_q \rangle$ for $q \to 0$ obtained via finite-size scaling (inset) is compared with the prediction from Luttinger-liquid theory, and we find very good agreement over a wide range of interaction strengths. Symbol colors are used to indicate different interaction strengths.

where we have introduced a possible linear drift term $\delta \cdot t$ to confirm the consistency of the quadratic Luttinger-liquid theory for density wave excitations. The drift term can be obtained from

$$\frac{\pi \delta}{4\omega_a} = (I_1 - I_{1/2}) = (I_{3/2} - I_1) = \frac{1}{2}(I_{3/2} - I_{1/2}), \quad (11)$$

and for all values of $q < k_{\rm F}$, we find $|\delta|/J \leqslant 2 \times 10^{-4}$, justifying the LL form of the static structure factor introduced in Eq. (3). We thus ignore any short-time drift in our subsequent analysis.

Next, we can similarly determine the q-dependent boson occupations from the I_n by combining

$$1 + 2\langle n_q \rangle = 2I_{1/2} - I_1 = \frac{1}{2}(3I_{1/2} - I_{3/2}) = 3I_1 - 2I_{3/2},$$
(12)

where in practice we determine $\langle n_q \rangle$ and its uncertainty as the average and standard error of the three different measurements. Finally, the prefactor of the oscillating term can be found from the extremal values at $t=0, \pi/2\omega_q, \pi/\omega_q$.

Thus, utilizing Eqs. (10)–(12) we extract $\langle n_q \rangle$, ω_q , and $\sinh(2\beta_q)$ from our exact diagonalization data (a numerical experiment). Performing finite-size scaling for each q and extrapolating to $q \to 0$, the LL boson occupation number can be computed as shown in Fig. 3 as a function of interaction strength. The success of this procedure can be independently confirmed by comparing the extracted values with those predicted from bosonization, $\langle n_{q\to 0} \rangle = (K+K^{-1}-2)/4$ using Eq. (9), which produces the solid line in Fig. 3. As can be seen, the agreement is excellent over a wide range of interaction strengths suggesting that the Luttinger parameter K could also be estimated in experiments using this procedure. With access to $\langle n_q \rangle$ we can now directly employ Eq. (6) to obtain the bosonic entropy.

Comparison with spatial entanglement entropy. This bosonic entropy can then be compared with the steady-state $(t \to \infty)$ value of the spatial entanglement entropy computed from Eq. (7). To this end, we determine the time dependence of the system's state after the quantum quench $|\Psi(t)\rangle$ via exact diagonalization and compute the reduced density matrix of a

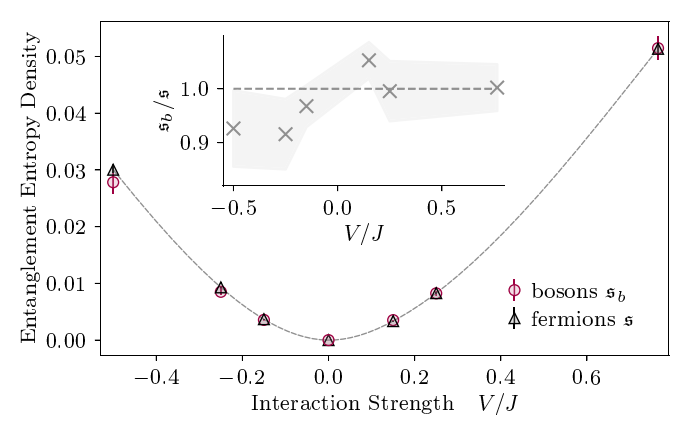


FIG. 4. Entanglement entropy density. We compare the steady-state spatial entanglement entropy density \mathfrak{s} for fermions with the entropy density \mathfrak{s}_b computed from a bosonic diagonal ensemble of density excitations Eq. (6). The bosonic occupation numbers $\langle n_q \rangle$ were obtained from an analysis of the data presented in Fig. 2. The dashed line is a guide to the eye. The ratio of the two entropy densities is consistent within error bars (inset).

subsystem of macroscopic size $\ell=L/2$ by tracing over half spatial modes available to the fermions. By applying the finite-size scaling and temporal extrapolation procedure described in a previous work by the authors [40], the density of the entanglement entropy $\mathfrak{s}\equiv\lim_{L\to\infty}\lim_{t\to\infty}S(t,L/2)/(N/2)$ can be obtained, where N/2 is the average number of particles in the spatial subregion. In Fig. 4 we show the comparison between the fermionic \mathfrak{s} and bosonic \mathfrak{s}_b entropy densities. The agreement is within error bars estimated from uncertainties in the two finite-size scaling procedures.

Conclusions. In this Letter, we have introduced a protocol to extract bosonic occupation numbers from the postquench time evolution of the static structure factor in a fermionic lattice model. Such a protocol could be implemented in current generation experiments of ultracold atomic gases via access to the density-density correlation function after a sudden change in the system. The resulting occupation numbers of bosonic density waves can be used to compute their entropy within a diagonal ensemble of noninteracting bosons. We compare this entropy with the exact steady-state entanglement entropy of the microscopic fermionic model under a spatial bipartition and find excellent agreement between the two. This provides evidence that the fluctuating degrees of freedom of the approximate Luttinger model and the exact Bethe ansatz solution contribute equivalently to the steady-state entropy density. While the model considered here is integrable, the method can be extended to include integrability breaking perturbations. In this case, any disagreement between the two entropies could indicate additional sources of entanglement generation and dynamics due to the reduction in conservation laws.

Acknowledgments. This work was supported in part by the NSF under Grants No. DMR-1553991 and No. 2041995 and the Deutsche Forschungsge-meinschaft (DFG) under Grants No. RO 2247/11-1 and No. 406116891 within the Research Training Group RTG 2522/1. A.D. expresses gratitude to the Institut für Theoretische Physik, Universität Leipzig for hospitality during the initial phase of this work.

- [1] P. Calabrese and J. Cardy, Evolution of entanglement entropy in one-dimensional systems, J. Stat. Mech. (2005) P04010.
- [2] A. M. Kaufman, M. E. Tai, A. Lukin, M. Rispoli, R. Schittko, P. M. Preiss, and M. Greiner, Quantum thermalization through entanglement in an isolated many-body system, Science 353, 794 (2016).
- [3] M. Srednicki, Chaos and quantum thermalization, Phys. Rev. E **50**, 888 (1994).
- [4] M. Rigol, V. Dunjko, V. Yurovsky, and M. Olshanii, Relaxation in a Completely Integrable Many-Body Quantum System: An *Ab Initio* Study of the Dynamics of the Highly Excited States of 1D Lattice Hard-Core Bosons, Phys. Rev. Lett. 98, 050405 (2007).
- [5] M. Rigol, V. Dunjko, and M. Olshanii, Thermalization and its mechanism for generic isolated quantum systems, Nature (London) 452, 854 (2008).
- [6] A. Polkovnikov, K. Sengupta, A. Silva, and M. Vengalattore, Colloquium: Nonequilibrium dynamics of closed interacting quantum systems, Rev. Mod. Phys. 83, 863 (2011).
- [7] L. F. Santos, A. Polkovnikov, and M. Rigol, Entropy of Isolated Quantum Systems after a Quench, Phys. Rev. Lett. 107, 040601 (2011).
- [8] B. Dóra, A. Bácsi, and G. Zaránd, Generalized Gibbs ensemble and work statistics of a quenched Luttinger liquid, Phys. Rev. B 86, 161109(R) (2012).
- [9] V. Gurarie, Global large time dynamics and the generalized Gibbs ensemble, J. Stat. Mech. (2013) P02014.
- [10] L. Piroli, E. Vernier, P. Calabrese, and M. Rigol, Correlations and diagonal entropy after quantum quenches in XXZ chains, Phys. Rev. B **95**, 054308 (2017).
- [11] E. Altman, E. Demler, and M. D. Lukin, Probing many-body states of ultracold atoms via noise correlations, Phys. Rev. A **70**, 013603 (2004).
- [12] E. D. Kuhnle, H. Hu, X.-J. Liu, P. Dyke, M. Mark, P. D. Drummond, P. Hannaford, and C. J. Vale, Universal Behavior of Pair Correlations in a Strongly Interacting Fermi Gas, Phys. Rev. Lett. 105, 070402 (2010).
- [13] M. Boll, T. A. Hilker, G. Salomon, A. Omran, J. Nespolo, L. Pollet, I. Bloch, and C. Gross, Spin-and density-resolved microscopy of antiferromagnetic correlations in Fermi-Hubbard chains, Science 353, 1257 (2016).
- [14] T. L. Yang, P. Grišins, Y. T. Chang, Z. H. Zhao, C. Y. Shih, T. Giamarchi, and R. G. Hulet, Measurement of the Dynamical Structure Factor of a 1D Interacting Fermi Gas, Phys. Rev. Lett. 121, 103001 (2018).
- [15] P. Calabrese and J. Cardy, Entanglement entropy and quantum field theory, J. Stat. Mech. 2004, P06002 (2004).
- [16] A. J. Daley, H. Pichler, J. Schachenmayer, and P. Zoller, Measuring Entanglement Growth in Quench Dynamics of Bosons in an Optical Lattice, Phys. Rev. Lett. 109, 020505 (2012).
- [17] R. Islam, R. Ma, P. M. Preiss, M. E. Tai, A. Lukin, M. Rispoli, and M. Greiner, Measuring entanglement entropy in a quantum many-body system, Nature (London) 528, 77 (2015).
- [18] M. A. Cazalilla, Effect of Suddenly Turning on Interactions in the Luttinger Model, Phys. Rev. Lett. 97, 156403 (2006).
- [19] A. M. Läuchli and C. Kollath, Spreading of correlations and entanglement after a quench in the one-dimensional Bose-Hubbard model, J. Stat. Mech. (2008) P05018.
- [20] J. Sabio and S. Kehrein, Sudden interaction quench in the quantum sine-Gordon model, New J. Phys. 12, 055008 (2010).

- [21] E. Ilievski, J. De Nardis, B. Wouters, J.-S. Caux, F. H. L. Essler, and T. Prosen, Complete Generalized Gibbs Ensembles in an Interacting Theory, Phys. Rev. Lett. **115**, 157201 (2015).
- [22] V. Alba, Eigenstate thermalization hypothesis and integrability in quantum spin chains, Phys. Rev. B **91**, 155123 (2015).
- [23] F. H. L. Essler and M. Fagotti, Quench dynamics and relaxation in isolated integrable quantum spin chains, J. Stat. Mech. (2016) 064002.
- [24] V. Alba and P. Calabrese, Entanglement and thermodynamics after a quantum quench in integrable systems, Proc. Natl. Acad. Sci. USA 114, 7947 (2017).
- [25] D. Jansen, J. Stolpp, L. Vidmar, and F. Heidrich-Meisner, Eigenstate thermalization and quantum chaos in the Holstein polaron model, Phys. Rev. B 99, 155130 (2019).
- [26] J. von Delft and H. Schoeller, Bosonization for beginners refermionization for experts, Ann. Phys. 7, 225 (1998).
- [27] T. Giamarchi, Quantum Physics in One Dimension (Oxford University Press, Oxford, UK, 2004)
- [28] See Supplemental Material at http://link.aps.org/supplemental/ 10.1103/PhysRevResearch.4.L022023 for more details on the bosonization calculation of the time evolution of the static structure factor.
- [29] F. D. M. Haldane, "Luttinger liquid theory" of one-dimensional quantum fluids. I. Properties of the Luttinger model and their extension to the general 1D interacting spinless Fermi gas, J. Phys. C 14, 2585 (1981).
- [30] K. V. Samokhin, Lifetime of excitations in a clean Luttinger liquid, J. Phys.: Condens. Matter 10, L533 (1998).
- [31] R. G. Pereira, J. Sirker, J.-S. Caux, R. Hagemans, J. M. Maillet, S. R. White, and I. Affleck, Dynamical Spin Structure Factor for the Anisotropic Spin-1/2 Heisenberg Chain, Phys. Rev. Lett. 96, 257202 (2006).
- [32] A. Del Maestro and I. Affleck, Interacting bosons in one dimension and the applicability of Luttinger-liquid theory as revealed by path-integral quantum Monte Carlo calculations, Phys. Rev. B 82, 060515(R) (2010).
- [33] A. Iucci and M. A. Cazalilla, Quantum quench dynamics of the Luttinger model, Phys. Rev. A **80**, 063619 (2009).
- [34] B. Dóra, M. Haque, and G. Zaránd, Crossover from Adiabatic to Sudden Interaction Quench in a Luttinger Liquid, Phys. Rev. Lett. 106, 156406 (2011).
- [35] J.-S. Caux and R. M. Konik, Constructing the Generalized Gibbs Ensemble after a Quantum Quench, Phys. Rev. Lett. **109**, 175301 (2012).
- [36] C. N. Yang and C. P. Yang, Thermodynamics of a one-dimensional system of bosons with repulsive delta-function interaction, J. Math. Phys. 10, 1115 (1969).
- [37] J. D. Cloizeaux, A soluble Fermi-gas model. Validity of transformations of the Bogoliubov type, J. Math. Phys. **7**, 2136 (1966).
- [38] C. N. Yang and C. P. Yang, One-Dimensional Chain of Anisotropic Spin-Spin Interactions. I. Proof of Bethe's Hypothesis for Ground State in a Finite System, Phys. Rev. 150, 321 (1966).
- [39] All code, scripts and data used in this work are included in a GitHub repository: https://github.com/DelMaestroGroup/papers-code-QuenchStructureFactorEntanglement, doi: 10.5281/zenodo.5679241.
- [40] A. Del Maestro, H. Barghathi, and B. Rosenow, Equivalence of spatial and particle entanglement growth after a quantum quench, Phys. Rev. B **104**, 195101 (2021).